Title: Spatio-temporal Variation in Aerial Arthropod Abundance Revealed by Weather Radars

Authors: Mansi Mungee[1], Maryna Lukach[2], Chris Shortall[3], James R. Bell[3,5], Elizabeth J. Duncan[4], Freya Addison[2], Lee E. Brown[1], William E. Kunin[4], Christopher Hassall[4], Ryan R. Neely III[2]*

Affiliations:

[1]School of Geography and water@leeds, Faculty of Environment, University of Leeds, Leeds, LS2 9JT, UK

[2]National Centre for Atmospheric Science, University of Leeds, Leeds, LS2 9PH, UK

[3]Rothamsted Insect Survey, Protecting Crops and the Environment, Rothamsted Research, Harpenden, AL5 2JQ, UK

[4]School of Biology, Faculty of Biological Sciences, University of Leeds, Leeds, LS2 9JT, UK

[5]Centre for Applied Entomology, Parasites and Pathogens, School of Life Sciences, Huxley Building, Keele University, Keele. ST5 5DX

***Corresponding author:** Ryan R. Neely III

Email: R.Neely@leeds.ac.uk

Author Contributions:

Methodology: MM, ML, RRN, CH, CS, JB, LEB; Visualization: MM, ML; Writing – original draft: MM, CH; Writing – review & editing: MM, ML, CS, JB, LEB, EJD, FA, WEK, CH, RRN Conceptualization: CH, RRN, EJD, WEK, JB; Investigation: CH, RRN, WEK, LEB, JB; Validation: CS, JB; Funding acquisition: WEK, CH, EJD, JB, LEB, RRN; Project administration: RRN, WEK, JB, CH; Supervision: RRN, CH, JB, LEB

Competing Interest Statement: Authors declare that they have no competing interests.

Classification: Biological Sciences, Ecology

Keywords: arthropod declines, radar entomology, spatio-temporal ecology, United Kingdom, weather radars

This file includes:

Abstract

Arthropod declines have been reported widely; however, a lack of comprehensive data has hindered our ability to assess their large-scale generality and drivers. Here, we used a novel and freely available dataset – atmospheric scans from a network of meteorological radars – to quantify aerial abundance of both diurnal and nocturnal arthropods across the United Kingdom, spanning different geographic regions and land cover types. Based on observations between 2014 and 2021, and across more than 35,000 km², we estimate numbers of arthropods flying over the UK at heights between 500 and 700 meters above ground at 1.12 (± 0.01) x 10^{13} individuals during the diurnal (0800–1400 UTC) and 5.02 (± 0.01) x 10^{12} during the nocturnal (including dusk, 1800–2200 UTC) period, showing significant spatial heterogeneity. Although spatial patterns differed, both diurnal and nocturnal arthropods increased in the south and declined mainly in the far north; on average, only nocturnal arthropods showed an overall decline. Aerial abundance of both diurnal and nocturnal arthropods showed positive relationships with woodland, grassland, and urban landcover, and negative relationships with artificial light intensity and arable landcover. Our study highlights the importance of spatial variation in temporal biodiversity trends and illustrates the need for comparative studies between nocturnal and diurnal arthropods. Notably, by extracting vertical profiles of radar reflectivity and polarization signatures, we demonstrate how weather radar datasets can be used to quantify aerial arthropod abundance, detect diurnal and seasonal activity patterns, and examine their environmental drivers across large spatial and temporal scales.

Significance Statement:

Evidence of alarming declines in arthropod numbers has been reported from sites across multiple countries worldwide, but we lack rigorous data to assess the generality, severity, and potential causes of such declines at large spatial and temporal scales. We use weather radars as an effective tool for large-scale monitoring of aerial arthropods across the United Kingdom and showed that on average, nocturnal arthropods showed a decline in abundance, while diurnal arthropods did not exhibit a significant decrease over an 8-year period (2014-2021). Widespread spatial variation in temporal trends for both diurnal and nocturnal arthropods were driven by light pollution intensity, habitat type, and climate. Radar monitoring of aerial arthropods offers unprecedented new insights into the abundance dynamics of aerial arthropods in space and time, offering exciting prospects for continental or global biodiversity monitoring in future, facilitating a new understanding of biodiversity loss.

Introduction

Arthropods dominate terrestrial, freshwater and aerial environments, making up 80% of known species (Bar-On et al. 2018). There have been increasing reports of declines in arthropod (and specifically insect) populations from around the globe, but the generality of this phenomenon including its rate, magnitude and extent remains poorly understood across large spatial and temporal scales (Simmons et al. 2019). Arthropods are a hyper-abundant and hyper-diverse group, and current monitoring methods are limited by high costs and restricted spatial and taxonomic coverage (Montgomery et al. 2020). Furthermore, the diverse metrics used to assess declines, such as species richness, occupancy, biomass, and abundance, are not directly comparable, presenting challenges to interpret and respond to the wide variability of reported trends (Didham et al. 2020). Notably, alarming trends have primarily been reported in total biomass and abundance, which are critical as they strongly impact ecosystem services (Hallman et al. 2017). This raises severe concerns among scientists and policymakers because arthropods play crucial roles in ecosystems as pollinators, decomposers, and as a vital food source for numerous organisms higher up in the trophic web (Losey & Vaughan 2006). Enhanced understanding of drivers and consequences of arthropod declines at large scales is therefore essential for developing effective conservation strategies and mitigating potential ecological and societal disruptions.

Empirical studies show that arthropods are affected by many different and interacting aspects of their environment such as climate, land cover change, invasive species, insecticides, and light pollution (Kehoe et al. 2021). However, much of our understanding about the relative effects of these drivers comes from studies either local in scale (e.g. point sampling), or utilizing presence-only occupancy records, or by employing space-for-time substitution (Blüthgen et al. 2022). Few studies have simultaneously compared temporal trends in arthropod abundances across multiple different habitat types and across large spatial extents (Bell et al. 2020; Uhler et al 2021). Nonetheless, understanding these relationships is critical for conservation strategies aiming to mitigate biodiversity loss (Wagner 2020).

Radar-based monitoring is an established tool for studying aerial animals and may provide a robust methodology for large-scale, standardized arthropod monitoring (Bauer et al. 2017). Most recent studies have used Vertical Looking Radars (VLR), which have generated considerable insights into aerial arthropod movement and abundance (Hu et al. 2016; Knop et al. 2023), but which provide limited spatial coverage. On the other hand, Weather Surveillance Radars (WSRs), intended to monitor meteorological phenomena, use existing infrastructure without extra costs, and provide unprecedented spatial coverage over thousands of square kilometers for broadscale biodiversity monitoring (Dokter et al. 2018). For example, the North American NEXRAD WSR network has been used to generate biologically meaningful data on bird phenology (Schools et al. 2012), migration (Schools et al. 2012; Sivakumar et al. 2021), demography (Nilsson et al. 2021), and epidemiology (McCuen et al. 2021) at national scales. With the advent of dual-polarization capabilities, where radars transmit and receive both horizontal and vertical pulses to distinguish the elongated shapes of insects from the more spherical signatures of precipitation, WSR networks have also been used to map the emergence and migration of arthropods (Boulanger et al. 2017; Stepanian et al. 2020).

Here, we demonstrate how observations from a national network of WSRs can be used to provide robust quantitative estimates of aerial arthropod abundance across vast spatial scales and at high temporal (twice a day) frequencies. We analyzed 8 years of data (2014-2021) from 15 WSRs (Fig. 1A) spanning more than 35,000 km^2 and 10° in latitude, and which represented a diverse variety of habitat types including woodland, agricultural and urban areas over which insects and other arthropods flew or were transported. We derived sub-daily data describing abundance trends across the UK, making it the most comprehensive spatial investigation for both diurnal and nocturnal arthropods using a common method. The resulting datasets were used to answer three primary questions: (i) what is the abundance of aerial arthropods across the UK? (ii) have there been significant changes in abundances over the studied time period? and (iii) what are the likely spatio-temporal drivers of any changes? We validate our analysis using long-term, standardized monitoring of aerial arthropod abundance from a suction trap situated close to a WSR station. Our approach provides a benchmark for directing future research efforts towards the long-term and

broad-scale investigation of overall arthropod abundance patterns using standardized, homogeneous, and openly available datasets at an unprecedented spatial scale and temporal resolution.

Materials and methods

1. UKMO radar network

The UK Met Office (UKMO) operates a network of 15 weather surveillance Doppler radars which provide complete airspace coverage over England, Wales, Scotland, and Northern Ireland (Fig. 1A) (Met Office 2003). Each Doppler radar is a C-Band (wavelength (λ) ≈ 5.3 cm), dual-polarization, monostatic radar which provides near-continuous polarimetric measurements of differential reflectivity (ZDR), co-polar correlation coefficient (ρHV) and phase differential (ΦDP), along with the standard legacy variables of single polarized radars, i.e., reflectivity factor (Z) and radial velocity (V). The raw polarimetric data from each radar are freely available from the Centre for Environmental Data Analysis archive in the form of HDF5 files (http://catalogue.ceda.ac.uk/uuid/82adec1f896af6169112d09cc1174499) (Met Office 2003). Ecological application of weather radar, especially for birds, has been the subject of several previous works (Schools et al. 2012; Boulanger et al. 2017; Dokter et al. 2018; Stepanian et al. 2020; Sivakumar et al. 2021; Nilsson et al. 2021), and therefore here we have only aimed to describe the unique specifications of the UKMO radars.

The raw data are disseminated in the form of Plan Positional Indicator (PPI) scans – i.e., a single 360° (azimuthal) scan carried out for a fixed elevation angle and repeated over a series of different angles. The PPIs are averaged to 600 m range gates and 1° in azimuth, close to the radar beam width of 1.1°. However, for our ecological analysis, we were interested in observing the data at a fixed azimuth and over multiple elevations i.e., at a fixed location in spatial coordinates and across different heights over that location. We generated Columnar Vertical Profiles (CVPs; described below) of all polarimetric variables using PPI scans from different elevation angles (typically between 0.5 and 4.0 degrees) sampled on Long Pulse mode (pulse length= 2.0 µs; range covered = 250 km) and with a 600 m gate resolution every 5 minutes.

2. Columnar Vertical Profiles (CVPs)

CVPs – 4D slices of data represented with latitude, longitude, time, and height – were generated following the approach of Murphy et al. (2020). Data from within the 600 m × 1° sectors were azimuthally averaged and projected to the CVP center, resulting in a vertical profile. The mean values were assigned as the profile value for different height bands, each 200 m deep (between 100 and 2100 m). Although, technically speaking, columns are not circular and not strictly vertical, for simplicity and homogeneity of calculations, a circular representation is selected. Cylindrical columns can be considered as the volume representing a subset of voxels (i.e. volume pixels). We chose a column radius of 2.5 km, and a vertical resolution (step-size or height) of 200 m as the optimum trade-off between sector size and step size, which facilitates uniform data averaging and projection (more details on CVP calculation and this selection criterion are discussed in *Supporting Information: Section S1*). This approach allows us to examine fine-scale variation in polarimetric variables (to within a 2.5 km horizontally and 200 m in height), and consequently in arthropod densities. This level of detail can be valuable for identifying the environmental drivers behind the observed variations.

For each radar, we generated 144 CVPs arranged in a 12 × 12 grid within a 60 km × 60 km bounding box, centered on the radar's coordinates (Fig. 1B). This spatial extent was chosen because radar sensitivity declines beyond 30 km, often requiring ad-hoc corrections that are unreliable for detecting sparse populations of small insects. Within a 30 km radius, the radar beam's vertical resolution is adequate for estimating abundance across discrete height bands (Kilambi et al. 2018). Applying this protocol across all 15 weather surveillance radars (WSRs) yielded a total of 2,160 CVPs (144 per radar). One CVP in the upper right corner (Fig. 1B) could not be processed for any radar due to technical limitations, leaving 2,145 CVPs for downstream processing.

As mentioned above, within a CVP, data from multiple elevation angles are azimuthally averaged and projected to the CVP centre. However, due to the radar beam angle and beam broadening, the

number of voxels at different heights vary with the range. We therefore removed 16 central CVPs (4 x 4 grid around the radar; Fig. 1B), where few or no voxels could be surveyed at greater heights. This resulted in a loss of data but did not bias our results, as it affected the same locations across all radars, and the number of CVPs per radar remained constant. We also removed additional CVPs for which an obstruction in the radar beam would result in severe ground clutter and shadowing, which can lead to issues when extracting comparatively weak arthropod echoes. Because obstructions caused by hills are typically long-lasting, we used a UK wide, 90 m Digital Terrain Model (DTM) to further remove 84 CVPs across different WSRs in which potential sources of obstruction were identified (Zrnic & Ryzkhov 1998; *Supporting Information: Section S1*). The final dataset thus consisted of *(127 * 15) - 84 = 1,821* CVPs in total. With the spatial area under each *CVP = 19.62 km^2 (π * 2.5^2),* this resulted in a complete spatial coverage of 35,728 km^2 across the UK (~15% of the country's area) above which aerial arthropod abundances were estimated.

3. CVP processing

We removed all meteorological signals that could be attributed to precipitation using the 'DR-Filtering' method developed by Kilambi et al. (2018). A depolarization ratio (DR) was calculated using polarimetric variables ZDR and ρHV, and all data below a DR threshold of −12.5 dB were identified as precipitation and removed (Kilambi et al. 2018; Stepanian et al. 2020). We also removed all data with extremely high reflectivity factors (>45 dBZ) which are often associated with heavy rainfall but may not be efficiently captured by the depolarization ratio (Kilambi et al. 2018; Fig. S1). We used differential reflectivity (ZDR) to remove all birds from the resulting data. High positive values of ZDR can be generally attributed to arthropods due to their somewhat more elongated body plans, with values ranging between 2 and 10 dB commonly observed (Zrnic & Ryzkhov 1998; Dokter et al. 2011; Melnikov et al. 2015; Stepanian et al. 2020; Mäkinen et al. 2022). For example, Dokter et al. (2011) used a threshold of 3 dB to filter out arthropods for studying bird migrations; for the decidedly more elongate mayflies, Stepanian et al. (2020) used a ZDR threshold of 5 dB. For UK arthropods, we used a conservative threshold of 3 dB to reduce co-occurring bird signatures.

We used seasonal and diurnal truncations to restrict our data to periods of known high arthropod activity across the country, which would further increase the signal to noise ratio for arthropods against birds. Arthropods, especially insects, are common in weather radar scans across the UK from late April to early October when warm and dry weather prevails. During this extended period, their aerial abundance generally peaks twice per day: a diurnal peak around midday and a dusk/nocturnal peak in the evening, typically shortly after sunset (Hu et al. 2016). To identify more specific start and end periods for these peaks within a year, and within a day, we used annual and diurnal time series profiles of ZDR. Data from all 15 WSRs were used to generate two distinct categories of time series profiles: annual time series with a daily resolution, and a daily time series with hourly resolution. Using non-linear Generalized Additive Models (GAMs), we selected a seasonal time window between 15th April to 30th October with peaks in ZDR (corresponding to higher density of horizontally elongated targets i.e., arthropods; Section S6) and truncated the data to only this period for estimating arthropod abundances (Fig. S2). Using a similar approach, we identified two different time windows within each day: 0800 to 1400 hrs. and 1800 to 2200 hrs GMT corresponding to maximum daily ZDRs (Fig. S2). To avoid repeatedly counting the same insects, we restricted our analysis to a single scan (with maximum ZDR) per time window, resulting in two abundance estimates – referred to as diurnal and nocturnal, respectively – per day between 15th April and 30th October. Selecting only one scan per time window also ensures that the unequal temporal coverage of 6 hours during diurnal and 4 hours during nocturnal does not bias the downstream modelling. The nocturnal scan window may overlap with civil twilight or daylight hours, potentially capturing dusk take-offs in addition to nocturnal flights. This overlap was accepted to maintain a standardized approach and to capture aerial arthropod abundance in a consistent and comparable manner across latitudes and months.

4. Estimating aerial arthropod abundance

Columns are approximated as cylinders for the calculation of all mean polarimetric variables at different height bands within a CVP. Therefore, arthropod abundance estimates discussed throughout the text correspond to the volume density within a single “CVP band”, i.e., estimated abundance per km^3 of atmosphere between specific height intervals of 200 m depth and referred

by the lower limit (e.g. abundance density at 500 m corresponds to the mean estimated abundance/km^3 of atmosphere between 500 and 700 m, and so on).

To estimate abundances at different heights, we adopted the methods developed by Chilson et al. (2012). We converted the radar reflectivity factor (Z) to the more biologically meaningful radar reflectivity (η) using the equation: η (dB) = Z (dBZ) + β, where β = 26.58 for the UKMO C-Band wavelengths (Chilson et al. 2012). The total (mean) reflectivity (in units of decibels) from each height band within a CVP, was then converted to linear units (cm^2/km^3), and multiplied by the total volume of a CVP band (km^3; $V_h = \Pi * r^2 * h$, where r = 2.5 km and h = 0.2 km) to obtain the total back-scattering area (cm^2) i.e., the total reflective surface from all arthropods within a CVP band. By dividing the total back-scattering area by the estimated mean Radar Cross Section (σ) of a single arthropod, we derived the total number of arthropods across different heights (Chilson et al. 2012; Stepanian et al. 2020) (see *Supporting Information: Section S2* for more information on how σ was estimated). Dividing this number again by V_h, we obtained the volume density within a single CVP band. All estimates correspond to the reflectivity from a single radar scan per diurnal and nocturnal time period (the scan with a maximum value of ZDR within each period). This approach avoided double counting of individuals that take flights more than once or that remain airborne in the same volume of air over an extended period of time per diurnal or nocturnal time window.

5.Validation Using Long-term Arthropod Monitoring Data

For validation of the estimated abundances, we used concurrent samples from a suction trap maintained by the Rothamsted Insect Survey (Bell et al. 2020), which is within the scan radius of Chenies weather radar (~17.6 km from the suction trap). Using the approach discussed above, we estimated aerial arthropod abundances for different heights above the location of the suction trap. We used Ordinary Least Squares (OLS) regression to assess the relationship between the observed daily arthropod abundances near the ground (from the suction trap data), and the abundance estimates obtained from the CVPs at different heights above the trap.

6.Statistical analysis

To model spatio-temporal variation in aerial arthropod abundance, we focused on estimates from a single band at 500 m, which was represented in the maximum number of CVPs per radar (lower bands at 100 and 300 m were not available for all CVPs due to radar beam angle (also see *Supporting Information: Section S4*; results for other heights are discussed in Section S5).

We assessed variation in the aerial arthropod abundance along spatial, temporal, and environmental variables, using a generalized additive modeling (GAMs) framework (Wood 2011; Wood 2017). GAM is an additive modeling technique where the impact of the different predictor variables is captured through non-linear, additive smoothing functions using the general form: $g(\mu) = \beta + \Sigma_{(j=1)}^{n} f_j(x_j)$, where the mean response (μ) is related to the predictor variables (x_1,….,x_n) by the identity link function *g(μ)* which defines the relationship between the response and '*n*' additive predictors. *β* represents the intercept term, and f_j is a smoothing function for the predictor x_j. Since our estimates of abundance were not derived from individual counts but total reflectivity on a continuous scale, we used Gaussian error distributions to model the estimated abundances instead of the commonly used Poisson for abundance counts. All GAMs were fitted using the R package '*mgcv' (Wood 2011)*, and the function "*bam*" with discrete = TRUE option for the large dataset.

Using the estimated arthropod abundance densities between 500 and 700 m as the response variable (μ), a total of 7 hierarchical spatio-temporal GAMs were fitted to the diurnal and nocturnal datasets independently (Table S1). The covariates (maximum daily temperature (Tmax), Rain, Wind, Artificial Light at Night (ALAN), Elevation, percentage land cover under Arable, Woodland, Grassland, and Urban (built-up areas + gardens) categories, Year, and the Latitude (y) and Longitude (x) of each CVP centroid, were fitted with thin-plate regression splines (*Supporting Information: Section S3*). As GAMs use shrinkage to reduce overfitting, the predictor "Year" only contributes the effect not represented by climate and land cover data. This minimises the probability of wrongly detecting a trend over time that could be attributed to variation in these environmental variables. We included CVP Grid location within the 12x12 lattice (Fig. 1B), Month, and Radar as random effects. Overall temporal trends in abundance were assessed by using the

305 modelled predictions averaged across all CVPs for each year, while complete spatio-temporal
306 predictions are based on all significant covariate relationships.
307
308 Given the large parameter space, we performed an automated variable selection using the 'double
309 penalty approach', implemented via the argument *select = TRUE* in *mgcv*. This approach adds an
310 additional, second penalty that allows shrinkage of the model linear terms, and therefore when
311 added to the first 'wiggliness' penalty, the two can result in an insignificant covariate being entirely
312 removed from the model. The best model was selected using a combination of model diagnostics
313 (normality and spread of the residuals, k-index (Wood 2011), deviance explained, ΔAIC and adj-
314 R^2), and AIC scores. We accounted for spatial autocorrelation by including smooth functions of the
315 individual CVP coordinates, i.e. *f(x,y)*, and for temporal autocorrelation using AR(1) autoregressive
316 function with the value of temporal autocorrelation parameter '*Rho'* estimated using the function
317 *start_value_rho()* from package *itsadug* (Rij et al. 2015). Residual spatial autocorrelation (patterns
318 in residuals correlated to spatial proximity) was evaluated using correlograms based on Moran's I
319 (Wood 2003), using CVP centroids as the spatial coordinates. Model fit was evaluated using the
320 *gam.check()* function in *mgcv*.
321
322 We used the function *predict.gam()* which enables a fitted gam model object to be used for
323 prediction at different values of the model covariates. We also used *predict.gam()* to estimate the
324 (approximate) uncertainty (standard errors) of those predictions obtained by the Taylor expansion
325 approach. These spatio-temporal predictions were used to generate yearly spatial maps of aerial
326 arthropod abundances per km^3 of atmosphere. All statistical analyses were performed in the R
327 programming environment (version 4.3.0; R Core Team 2023) on Platform:x86_64-pc-linux-gun
328 (64-bit). Raw weather data retrieval, storage and CVP analyses were facilitated using JASMIN, the
329 UK's collaborative data analysis environment (https://jasmin.ac.uk; Lawrence et al. 2013).
330
331 **Results**
332 **Arthropod abundance from weather surveillance radars**

Median arthropod density within the 500 m CVP band (i.e. abundance/km^3 between 500 and 700 m height) was 4.61 x 10^7 (interquartile range = 3.77 x 10^8) and 2.06 x 10^7 (interquartile range = 2.91 x 10^8) diurnal and nocturnal arthropods, respectively. Extrapolating this to the entire UK indicates that an average of 1.12 (± 0.01) x 10^{13} diurnal and 5.02 (± 0.01) x 10^{12} nocturnal arthropods were present over the UK between 500 and 700 m height, between 15th April and 30th October, and at any given instance between 0800 - 1400 and 1800 - 2200 GMT, respectively, although with high inter-annual variability (Fig. S3).

On average, arthropod abundances decreased monotonically at the rate of 8.74 (±0.01) x 10^5 individuals per 200 m of height gained in the air column (Diurnal: slope = -7.77 (± 0.01) x 10^5, *Adj. R^2 = 0.11, p < 0.001*; Nocturnal: slope = -9.71 (± 0.21) x 10^5, *Adj. R^2 = 0.12, p < 0.001*; Fig. S4).

Validation using long-term arthropod monitoring data

Based on the dual-polarization coverage of the Chenies weather radar, and the number of operational days at the Rothamsted suction trap, we obtained n = 127 days that overlapped across the two datasets. We further removed days (n = 9; entire day i.e., 24-hr removed) where heavy rainfall occurred, resulting in a total of 116 days for comparison. We found strong and significant correlations between estimated abundances and at different heights in the CVP with the observed arthropod abundances at 12.2 m suction traps (*Adj. R^2 = 0.32 to 0.47; p < 0.001; Fig. 2A*). As expected, the slope of this relationship decreased with height, with the strongest relationship at lowest height (Fig. 2A).

Spatio-temporal variation

Of the 7 hierarchical GAMs tested (Table S1), the best fitting model included the following terms:

$$g(\mu) = f1(year) + f2\left(year_f, R\right) + f3(radar, R) + f4(Year, by = Radar) +$$

$$f5(month, R) + f6(CVP_{location}, R) + f7(x, y)$$

along with the following 9 covariates:

$$f8(Tmax) + f9(Rain) + f10(Wind) + f11(Arable) +$$

$$f12(Urban) + f13(Woodland) + f14(Grassland) + f15(ALAN) + f16(Elevation)$$

This model explained 80.2% and 76.4% of the total deviance in diurnal and nocturnal arthropods respectively and revealed significant spatio-temporal heterogeneity across the WSR network (Table S2 & S4). Average cumulative predictions per year revealed significant declines in nocturnal arthropod abundances over time; however, diurnal abundances did not exhibit a consistent negative trend with year (Fig. 3A). Nearly all the tested variables had similar patterns of associations with both diurnal and nocturnal arthropod populations, indicating a broad scale generality of the relationships (Fig. 3B-G). The only variable showing different effects on diurnal and nocturnal arthropods was ALAN, which had a weak negative effect on nocturnal species, and a strong negative effect on diurnal ones, but only at higher ALAN levels. Woodland and grassland cover had positive associations (Fig. 3F & 1G), while arable cover revealed a negative relationship with aerial arthropod abundances but only for high arable land cover (Fig. 3D). Across the individual, height-stratified GAMs, the estimated effect sizes (and significance) of land cover covariates declined progressively with increasing height (*Supporting Information: Section S5*).

Arthropod abundances showed a strong spatial dependence, with a significant effect of the smoothed terms for the CVP's x and y coordinates [$f_7(x,y)$], and the temporal trends exhibited a higher net decline towards the higher latitudes, for both diurnal and nocturnal arthropods (Fig 4). We also observed an increase (positive change) in arthropod abundances at the lower latitudes (Fig 4). The modelled relationship between abundance and all covariates was used to generate national scale spatio-temporal predictions for new, un-sampled locations (Fig. 5).

Discussion

By employing an extensive and standardized dataset on a national scale, our study has revealed important broadscale spatio-temporal patterns in the abundance of aerial arthropods across the UK between 2014 and 2021. On average, nocturnal arthropods showed a decline in abundance, while diurnal arthropods showed substantial inter-annual variation, but no overall increasing or

390 decreasing trend (Fig. 3A). However, these trends were not consistent across all regions: both
391 groups exhibited significant increases in abundance over the southern latitudes, with declines
392 primarily confined to the northernmost regions (Fig. 4). Our study emphasizes the significance of
393 spatial variation in obscuring temporal trends (Wagner et al.2021), which is likely important when
394 analyzing the impact of spatially structured drivers. Furthermore, we have demonstrated that WSR
395 networks can deliver systematic, non-invasive biodiversity monitoring which provides large-scale
396 and continuous coverage at high temporal resolutions.
397
398 Spatio-temporal variation indicated declines in arthropod abundance at higher latitudes across the
399 UK, compared to the south (Fig. 4B). The decline in the north reflects the observed negative
400 association between maximum daily air temperature (Tmax) and arthropod abundances which
401 were most prominent at lower values of Tmax typical of northern latitudes in the UK (Fig. 3B).
402 Temperature has increased in the UK over the study period (Christidis et al. 2023) and the positive
403 correlation between arthropod abundance and Tmax at higher values of the latter would also
404 explain the increase in the southern latitudes. Recent warming has been highly uneven across the
405 globe, with higher latitudes warming faster than the tropics (Intergovernmental Panel on Climate
406 Change (IPCC), 2021). However, the UKCP18 projections reveal the opposite latitudinal gradient
407 for the UK: maximum temperatures have risen (and are projected to rise) more sharply in southern
408 England than in northern Scotland (Lowe et al. 2018; Murphy et al. 2018). This north–south
409 asymmetry in warming, together with the positive correlation between arthropod abundance and
410 higher Tmax, would offer some explanation for why increases were concentrated in southern
411 CVPs, whereas declines were largely confined to the northernmost regions. These findings
412 underscore how spatial variation in climate change can drive contrasting temporal biodiversity
413 trends within a relatively small geographic area. Previous research has shown that distinct
414 atmospheric layers in aerial arthropods are associated with local maxima in the vertical air
415 temperature profile (Drake 1984; Wood et al. 2006), suggesting that the inclusion of finer-scale
416 variables (vertical profiles of local climate) is likely to improve the prediction of aerial arthropod
417 variability in radar datasets in future (e.g. UK Met Office's numerical weather prediction model, the
418 "Unified Model") (Brown et al. 2008).

Habitat type and land cover changes have been identified in the past as the main drivers of arthropod declines, a factor implicated equally in global bird and mammal declines (Chamberlain & Fuller (2000). While our samples are constrained to arthropods suspended in the atmosphere above the habitat matrix below, we did find associations with the different habitat types. We observed a negative relationship of aerial arthropod abundances with arable cover, and a positive relationship with woodland, grassland and, surprisingly, urban land cover. The negative effects of increasing arable cover are often mediated by loss of native plants, increased use of pesticides and fertilizers, increased frequency of harvest in recent years, and others, which are deemed to be key drivers of arthropod declines (Fox 2013). The strong positive effect of urban cover (Fig. 3E) may be due to urban heat island effects (Youngsteadt et al. 2017); arthropod aerial movements, particularly at higher heights, are triggered by steadily rising isothermal currents associated with warmer temperatures of urbanized regions (Reynolds et al. 2008). A similar observation was noted recently for birds (Van Doren et al. 2017). Although the pattern is contrary to expectation, it should be noted that 'urban cover' represents a broad, heterogeneous category spanning all built-up areas, gardens and suburban areas. Thus, a more detailed investigation into the relative abundances across these categories may provide a deeper understanding of the role of urban cover on aerial arthropod abundances. This positive association likely causes predictive modelling to show urban regions as the most prominent hotspots of aerial arthropod abundance across the UK (Fig. 5).

The predicted patterns of urban insect abundance differed markedly between nocturnal and diurnal arthropods, with nocturnal densities elevated throughout urban areas, while diurnal taxa show depressed abundance in urban centres. This suggests that the concentration of nocturnal arthropods in cities could at least partly be due to the attraction to ALAN, as shown previously for birds (Van Doren et al. 2017) and insects (Tielens et al. 2021). For example, urban areas of Las Vegas (USA) were previously characterized as a large-scale attractive sink on nocturnal flights of arthropod population, indicating the attractive or disorienting effect of artificial light (Tielens et al. 2021). ALAN impacts the vital biological functions of nocturnal and diurnal arthropods alike; it alters

448 the circadian patterns of activity and rest in diurnal arthropods which results in impaired immune
449 function, reduced fecundity, and a shorter lifespan (Kouser et al. 2014; Durrant et al. 2015) It also
450 causes diurnal and crepuscular arthropods to move their foraging activity into the night which
451 subjects them to increased predation (Garber 1978), and cold stress (Owens & Lewis 2018).
452 Despite a potentially negative effect on both nocturnal and diurnal arthropod populations, the
453 impact on nocturnal arthropods may be masked by positive density effects due to behavioural
454 attraction; nocturnal arthropods are drawn to light sources across larger distances (Owens & Lewis
455 2018). On the other hand, the negative fitness effects on demography should accumulate over time
456 via effects on arthropod circadian rhythms, navigation, and foraging behavior (Manfrin et al. 2017).
457 The stronger negative effect of very high ALAN values on diurnal arthropods in our findings is
458 counter-intuitive (Fig. 3C) and may be due to some other driving variable not considered in the
459 present analyses. Specifically, the very high ALAN intensities associated with reduced diurnal
460 arthropod abundances may be associated with core cities, and/or with industrial or transport
461 infrastructure, distinguishing them from suburban environments characterised by only moderate
462 ALAN levels. With temporal niche partitioning between diurnal and nocturnal species becoming
463 less extreme in response to human activity (Levy et al. 2019; Owens et al. 2020), more research is
464 needed to document the role of ALAN in arthropod declines, including diurnal groups/species. We
465 ensured that the diurnal effect of ALAN was independent of urban cover by re-running our models
466 after accounting for the correlation between ALAN and urban cover (*Supporting Information*
467 *Section S4*).
468
469 As previously mentioned, all spatio-temporal patterns and predictions discussed here correspond
470 to the arthropods within a specific height band in the atmosphere (between 500 – 700 m). Previous
471 work have shown that the median flight layer has remained altitudinally stable over the past
472 decade (Gao et al. 2020), and that there is strong temporal coupling among neighbouring (vertically
473 adjacent) layers (Reynolds et al. 2005). These observations suggest that a single, broad altitudinal
474 band provides a reliable index of (relative) spatio-temporal changes in aerial abundances of
475 arthropods. Although the vertical layering is strongly governed by temperature inversions,
476 boundary-layer depth and wind shear (Drake 1984; Reynolds et al. 2005), these phenomenon have

so far reported weak or non-monotonic long-term trends in previous studies (Zhang et al. 2013; Shahi et al. 2020; Yue et al. 2021). Nevertheless, future work linking height-resolved arthropod abundances with detailed, local temperature profiles and atmosheric processes will be essential to detect climate- and habitat-driven redistribution of flight heights. We analysed the land-cover relationship for estimated arthropod abundances at different heights and observed a diminishing influence of land cover variables with increasing height (*Supporting Information: Section S5*). Notably, aerial arthropods at heights greater than 900 m were not significantly correlated to a single land cover variable. This indicates that arthropods undertaking flights at higher heights are decoupled from the underlying habitat type, most likely because they are engaged in a longer distance flight, covering distances greater than our CVP spatial resolution. This is further supported by the large number of recent studies showing that even the tiniest aerial arthropods (e.g. aphids and micro-hymenopterans) are not entirely passive in their dispersal processes (Reynolds & Reynolds 2009; Wainwright et al. 2017; Ortega-Jiménez & Combes 2018; Bell & Shepherd 2024), and exhibit attraction to light sources (Kirchner et al. 2005; Döring & Chittka 2007). Future studies are needed to delve deeper into the size and taxonomic classifications of radar observations, providing clearer insights into how spatio-temporal trends translate to different ecological groups (Lukach et al. 2022).

Much of our macroscale understanding of arthropod diversity trends so far has been derived from studies on ground-dwelling and/or low-flying diurnal insects. Consequently, it is not unexpected that some of the emerging results – especially the positive association between urban land cover and aerial arthropod density, and the negative effect of ALAN on diurnal arthropods – are novel and counterintuitive. These observations show that aerial arthropods may not be temporally and/or spatially synchronised with arthropod activity at ground level and hence may not accord with the monitoring of field-caught species or the perceptions of those who collect them. It is also the case that these arthropods are almost entirely being monitored during one life stage – the adult winged phase, part of a much more complex life cycle which cannot be measured using radar. The importance of this study is to open a window to a huge and important new source of biodiversity monitoring data. Our findings here are just a tantalizing glimpse of what such data can reveal, and

506 further longer-term analyses should be conducted as these datasets grow longer, especially to
507 confirm the continuity of the temporal trends we detect.
508
509 Our work has provided significant insights into aerial arthropod activity, confirming and extending
510 findings initially observed with Vertical Looking Radars (VLRs; *Supporting Information Section S6*).
511 For instance, the positive correlation between differential reflectivity (ZDR) and aerial arthropod
512 density (Fig. 2B) is consistent with VLR observations of horizontally aligned targets at similar
513 heights. Peaks in ZDR between April and October, and during mid-day and evening, also validate
514 earlier observations of high insect activity during these windows (Hu et al. 2016). The extensive
515 scale of our results reveals the broadscale generality of these mechanisms across a range of
516 biomes.
517
518 A series of interesting research gaps emerge from our work. First, the taxonomic and/or
519 morphological resolution that can be derived from WSR observations requires further analysis.
520 Although current radar-based estimates of arthropod abundance are not species-specific
521 (Chapman et al. 2011; Hüppop et al. 2019; Gauthreaux & Diehl 2020; Bauer et al. 2024), recent
522 studies suggest that WSR data – especially when coupled with ground-based monitoring – has the
523 potential to discriminate among different biological taxa, at least at higher taxonomic levels (e.g.
524 Orders) (Lukach et al. 2022; Hu et al. 2024). There is a need for extensive work in electromagnetic
525 modeling and simulation to explore radar cross sections of a diverse array of arthropod taxa to
526 classify the radar data by broad taxonomic groups (Mirkovic et al. 2016; Mirkovic et al. 2019;
527 Addison et al. 2022). Our analyses here have assessed only overall arthropod numbers, but a
528 degree of morphological information concerning sizes and shapes is provided in dual-polarization
529 radar reflectance data. Future studies could be explicitly designed to bridge the gap between
530 ground-based long-term monitoring and weather radar observations; high-throughput tools such as
531 metabarcoding from suction trap samples, along with strategic new sampling approaches (e.g.,
532 drone-based aerial surveys), could help build the crucial taxonomic link between radar signals and
533 biological identity. Second, much of the research using radar has focused on migratory organisms
534 rather than resident populations. The relative contribution of migrants to local arthropod

communities, and, hence, the value of migration to the ecosystem services that are provided by those communities remain poorly understood. Incorporating data from citizen and community scientists, who increasingly contribute to species-level occurrence data and can measure near-ground abundances that are invisible to the WSR, particularly for moths and freshwater insects migrating along watercourses in the UK, could enhance our understanding of local arthropod communities and their ecological contributions. Addressing these issues will require collaborations between scientists, engineers, conservation practitioners, policymakers, and citizen scientists to advance the use of radar-derived measures in biodiversity conservation.

Our research is one of the first studies to empirically assess abundance changes and potential drivers to a broad-spectrum of aerial arthropod taxa at a national scale. Spatial heterogeneity has posed a significant challenge in reconciling temporal trends in arthropod declines, even within a single taxonomic group (Didham et al. 2020). Until now, it has remained uncertain whether observed heterogeneity stemmed from methodological disparities between studies or was an inherent characteristic of arthropod communities (Wagner 2020). The methods developed herein provide insights into both diurnal and nocturnal arthropod trends using a single monitoring method, something that is missing from contemporary monitoring methods. This analytical framework can be used to investigate how future changes in major environmental conditions may influence aerial arthropod densities. This is the first critical step for better understanding their roles in ecosystem functions and services.

The benefits of WSR observations come at relatively little marginal cost because the underlying infrastructure – comprising radar installations, data acquisition systems, and archival platforms – is already established and maintained through national meteorological services for operational weather forecasting. Unlike traditional arthropod monitoring methods, which often involve resource-intensive collection tools and incur significant field costs for data collection, weather radar data are continuously and passively collected at high spatio-temporal resolution. The primary costs associated with ecological use of radar data arise not from data acquisition but from data processing. These include maintenance of processing scripts and pipelines (1 person-month per

year; ~ £10,000 with full economic costing), storage and compute capacity (estimated at £10,000 to £30,000 annually depending on data volume and archival depth, though currently subsidized for NERC projects via platforms such as JASMIN), and updates to classification algorithms in response to changes in radar hardware or improvements in methodology (additional personnel; @ ~£10,000 per year). These are best viewed as fixed service-level costs, akin to community-wide resources like GBIF or GenBank, rather than project-specific expenses. Given the ubiquity of existing national WSR networks across Eurasia, the Americas and Australasia (and as well as the current expansion of networks globally), there are exciting prospects for continental or even global scale biodiversity monitoring in future.

Acknowledgments

UKRI Natural Environment Research Council NE/S001298/1 (CH, RRN, EJD, WEK); UKRI Natural Environment Research Council NE/W004534/1 (CH, RRN); UKRI Natural Environment Research Council NE/V006916/1 (WEK, CH, RRN, JB, LEB); Bill and Melinda Gates Foundation OPP1212006 (WEK, RRN, CH); Core Capability Grant BBS/E/C/000J0200. The Rothamsted Insect Survey, a National Bioscience Research Infrastructure, is funded by the Biotechnology and Biological Sciences Research Council under the award BBS/E/RH/23NB0006. We are grateful to the collaborators and staff who have contributed data from the Rothamsted Insect Survey. This work used JASMIN, the UK's collaborative data analysis environment *(https://jasmin.ac.uk)*. RN, EJD and CH would like to acknowledge the University of Leeds Crucible Programme, which provided support and funding for the early stages of the project and without which none of this work would have been possible.

Data and materials availability: All WSR data used here are freely available from CEDA (Centre for Environmental Data Analysis) Archive, which is a part of NERC's Environmental Data Service (EDS). The code to convert raw data into CVPs, and the scripts used for spatio-temporal models and predictions are available through a GitHub repository.

References

1. Y.M. Bar-On,R, Phillips, R. Milo, The biomass distribution on Earth. *Proceedings of the National Academy of Sciences* ***115***, 6506 – 6511 (2018)
2. B.I. Simmons, A. Balmford, A.J. Bladon, A.P. Christie, A. De Palma, L.V. Dicks, J. Gallego-Zamorano, A. Johnston, P.A. Martin, P. Andy, R. Rocha, H.S. Wauchope, F.R.C. Wordley, T.A. Worthington Finch, Worldwide insect declines: An important message, but interpret with caution. *Ecology and Evolution* ***9***, 3678 – 3680 (2019)
3. G.A. Montgomery, R. Dunn, R. Fox, E. Jongejans, S.R. Leather, M.E. Saunders, C.R. Shortall, M.W. Tingley, D. L. Wagner, Is the insect apocalypse upon us? How to find out. *Biological Conservation* ***241***, e108327 (2020)
4. R.K. Didham, Y. Basset, C.M. Collins, S.R Leather, N.A. Littlewood, M.H.M. Menz, J. Müller, L. Packer, M.E. Saunders, K. Schönrogge, J.A.A. Stewart, S.P. Yanoviak, C. Hassall, Interpreting insect declines: seven challenges and a way forward. *Insect Conservation and Diversity* ***13***, 103 – 114 (2020)
5. C.A. Hallmann, M. Sorg, E. Jongejans, H. Siepel, N. Hofland, H. Schwan, W. Stenmans, A. Müller, H. Sumser, T. Hörren, More than 75 percent decline over 27 years in total flying insect biomass in protected areas. *PloS one* ***12***, e0185809 (2017)
6. J.E. Losey, M. Vaughan, The economic value of ecological services provided by insects. *Bioscience* ***56***, 311 – 323 (2006)
7. R. Kehoe, E. Frago, D. Sanders, Cascading extinctions as a hidden driver of insect decline. *Ecological Entomology* ***46***, 743 – 756 (2021)
8. N. Blüthgen, M. Staab, R. Achury, W.W. Weisser, Unravelling insect declines: can space replace time? *Biology Letters* ***18***, e20210666 (2022)
9. J.R. Bell, D. Blumgart, C.R. Shortall, Are insects declining and at what rate? An analysis of standardised, systematic catches of aphid and moth abundances across Great Britain. *Insect Conservation and Diversity* ***13***, 115 – 126 (2020)
10. J. Uhler, S. Redlich, J. Zhang, T. Hothorn, C. Tobisch, J. Ewald, S. Thorn, S. Seibold, O. Mitesser, J. Morinière, Relationship of insect biomass and richness with land use along a climate gradient. *Nature Communications* ***12***, e5946 (2021)

11. D.L. Wagner, Insect Declines in the Anthropocene. *Annual Review of Entomology* ***65***, 457 – 480 (2020)
12. S. Bauer, J. Chapman, D.R. Reynolds, J.A. Alves, A.M. Dokter, M.H.M. Menz, N. Sapir, M. Ciach, L.B. Pettersson J.E. Kelly. From agricultural benefits to aviation safety: realizing the potential of continent-wide radar networks. *BioScience* ***67***, 912 – 918 (2017)
13. G. Hu, K. Lim, N. Horvitz, S.J. Clark, D.R. Reynolds, N. Sapir, J.W. Chapman, Mass seasonal bio flows of high-flying insect migrants. *Science* ***354***, 1584 – 1587 (2016)
14. E. Knop, L.G. Majken, K. Fränzi, S. Baptiste, F. Liechti, Patterns of high-flying insect abundance are shaped by landscape type and abiotic conditions. *Scientific Reports* ***13***, e15114 (2023).
15. A.M. Dokter, F. Andrew, F. Daniel, R. Viviana, W.M. Hochachka, F.A. La Sorte, O. J. Robinson, K.V. Rosenberg, S. Kelling. Seasonal abundance and survival of North America's migratory avifauna determined by weather radar. *Nature Ecology & Evolution* **2**, 1603-1609 (2018).
16. E.H. Schools, H.D. Enander, J.L. Gehring, B.J. Klatt, C.A. Forgacs, Utilizing NEXRAD Weather Data and a Hotspot Analysis to Determine Bird Migration Concentration Areas. *Michigan Natural Features Inventory Report* ***21,*** (2012).
17. A.H. Sivakumar, D. Sheldon, K. Winner, C.S. Burt, K.G. Horton, A weather surveillance radar view of Alaskan avian migration. *Proceedings of the Royal Society B: Biological Sciences* ***288***, e20210232 (2021)
18. C. Nilsson, F. La Sorte, A. Dokter, K. Horton, B.M. Van Doren, J.J. Kolodzinski, J. Shamoun-Baranes, A. Farnsworth, Bird strikes at commercial airports explained by citizen science and weather radar data. *Journal of Applied Ecology* ***58***, 2029 – 2039 (2021)
19. M.M. McCuen, M. Pitesky, J.J. Buler, S. Acosta, A.H. Wilcox, R.F. Bond, S.L. Díaz-Muñoz, A comparison of amplification methods to detect Avian Influenza viruses in California wetlands targeted via remote sensing of waterfowl. *Transboundary and Emerging Diseases* ***68***, 98 – 109 (2021)
20. Y. Boulanger, F. Fabry, A. Kilambi, D.S. Pureswaran, B.R. Sturtevant, R. Saint-Amant, The use of weather surveillance radar and high-resolution three dimensional weather data to

monitor a spruce budworm mass exodus flight. *Agricultural and Forest Meteorology* ***234***, 127 – 135 (2017)

21. P.M. Stepanian, S. Entrekin, C.E. Wainwright, D. Mirkovic, J.L. Tank, J.F. Kelly, Declines in an abundant aquatic insect, the burrowing mayfly, across major North American waterways. *Proceedings of the National Academy of Sciences* ***117***, 2987 – 2992 (2020)
22. Met Office (2003): Met Office Rain Radar Data from the NIMROD System. NCAS British Atmospheric Data Centre, http://catalogue.ceda.ac.uk/uuid/82adec1f896af6169112d09cc1174499
23. A.M. Murphy, A. Ryzhkov, P. Zhang, Columnar vertical profile (CVP) methodology for validating polarimetric radar retrievals in ice using in situ aircraft measurements. *Journal of Atmospheric and Oceanic Technology* ***37***, 1623 – 1642 (2020)
24. J.W. Chapman, V. Drake, D.R. Reynolds, Recent Insights from Radar Studies of Insect Flight. *Annual Review of Entomology* ***56***, 337 – 356 (2011)
25. A. Kilambi, F. Fabry, V. Meunier, A simple and effective method for separating meteorological from non-meteorological targets using dual-polarization data. *Journal of Atmospheric and Oceanic Technology* ***35***, 1415–1424 (2018)
26. A.M. Dokter, F. Liechti, H. Stark, L. Delobbe, P. Tabary, I. Holleman, Bird migration flight altitudes studied by a network of operational weather radars. *Journal of the Royal Society Interface* ***8***, 30 – 43 (2011)
27. T. Mäkinen, J. Ritvanen, S. Pulkkinen, N. Weisshaupt, J. Koistinen, Bayesian Classification of Non-meteorological Targets in Polarimetric Doppler Radar Measurements. *Journal of Atmospheric and Oceanic Technology* ***39***, 1561–1578 (2022)
28. D.S. Zrnic, A. Ryzhkov, Observations of insects and birds with a polarimetric radar. *IEEE transactions on geoscience and remote sensing* ***36***, 661–668 (1998)
29. V.M. Melnikov, M. Istok, J.K. Westbrook, Asymmetric radar echo patterns from insects. *Journal of Atmospheric and Oceanic Technology* ***32***, 659–674 (2015)
30. D.L. Harrison, S. J. Driscoll, M. Kitchen, Improving precipitation estimates from weather radar using quality control and correction techniques. *Meteorological Applications* ***7***, 135 – 144 (2000)

31. P.B. Chilson, W. Frick, P.M. Stepanian, J.R. Shipley, T.H. Kunz, J.F. Kelly, Estimating animal densities in the aerosphere using weather radar: To *Z* or not to *Z*?. *Ecosphere* ***3***, 1-19 (2012)
32. Wood, S.N. (2011) Fast stable restricted maximum likelihood and marginal likelihood estimation of semiparametric generalized linear models. Journal of the Royal Statistical Society (B) 73(1):3-36
33. S. N. Wood, *Generalized Additive Models: an introduction with R*. (CRC press, 2017)
34. van Rij J, Wieling M, Baayen R, van Rijn H (2022). “itsadug: Interpreting Time Series and Autocorrelated Data Using GAMMs.” R package version 2.4.1.
35. Wood, S.N. (2003) Thin-plate regression splines. Journal of the Royal Statistical Society (B) 65(1):95-114.
36. R Core Team (2023). _R: A Language and Environment for Statistical Computing_. R Foundation for Statistical Computing, Vienna, Austria. <https://www.R-project.org/>
37. Lawrence, B. N., Bennett, V. L., Churchill, J., Juckes, M., Kershaw, P., Pascoe, S., Pepler, S., Pritchard, M. and Stephens, A. (2013) *Storing and manipulating environmental big data with JASMIN.* In: IEEE Big Data, October 6-9, 2013, San Francisco.
38. Wagner, D. L., Fox, R., Salcido, D. M., & Dyer, L. A. (2021). A window to the world of global insect declines: Moth biodiversity trends are complex and heterogeneous. *Proceedings of the National Academy of Sciences*, *118*(2), e2002549117.
39. Christidis, N., Stott, P. A., & McCarthy, M. (2023). An attribution study of the UK mean temperature in year 2022.
40. V.A. Drake, The vertical distribution of macro-insects migrating in the nocturnal boundary layer: A radar study. Boundary-Layer Meteorology ***28***, 353 – 374 (1984)
41. C.R Wood, J. Chapman, D.R Reynolds, J.F. Barlow, A.D. Smith, I.P. Woiwod, The influence of the atmospheric boundary layer on nocturnal layers of noctuids and other moths migrating over southern Britain. *International Journal of Biometeorology* ***50***, 193 – 204 (2006)

42. Brown, A. R., R. J. Beare, J. M. Edwards, A. P. Lock, S. J. Keogh, S. F. Milton, and D. N. Walters. "Upgrades to the boundary-layer scheme in the Met Office numerical weather prediction model." *Boundary-layer meteorology* 128 (2008): 117-132.
43. D.E. Chamberlain, R. Fuller, Local extinctions and changes in species richness of lowland farmland birds in England and Wales in relation to recent changes in agricultural land-use. Agriculture, *Ecosystems & Environment* ***78***, 1 – 17 (2000)
44. R. Fox, The decline of moths in Great Britain: a review of possible causes. *Insect Conservation and Diversity* ***6***, 5 – 19 (2013)
45. E. Youngsteadt, A. Ernst, R.R. Dunn, S.D. Frank, Responses of arthropod populations to warming depend on latitude: evidence from urban heat islands. *Global Change Biology* ***23***, 1436 – 1447 (2017)
46. D.R. Reynolds, A. Smith, J.W. Chapman, A radar study of emigratory flight and layer formation by insects at dawn over southern Britain. *Bulletin of Entomological Research* ***98***, 35 – 52 (2008)
47. B.M. Van Doren, K. Horton, A.M. Dokter, H. Klinck, D.B. Elbin, A. Farnsworth, High-intensity urban light installation dramatically alters nocturnal bird migration. *Proceedings of the National Academy of Sciences* ***114***, 11175 – 11180 (2017)
48. E.K. Tielens, P. Cimprich, B.A. Clark, A.M. DiPilla, J.E. Kelly, D. Mirkovic, A.I. Strand, M. Zhai, P.M. Stepanian, Nocturnal city lighting elicits a macroscale response from an insect outbreak population. *Biology Letters* ***17***, e20200808 (2021)
49. J. Durrant, E. Michaelides, T. Rupasinghe, D. Tull, M.P. Green, T.M. Jones, Constant illumination reduces circulating melatonin and impairs immune function in the cricket Teleogryllus commodus. *PeerJ* ***3***, e1075 (2015)
50. S. Kouser, Palaksha, V. Shakunthala, Study on fitness of Drosophila melanogaster in different light regimes. Biological Rhythm Research ***45***, 293 – 300 (2014)
51. S.D. Garber, Opportunistic feeding behaviour of *Anolis cristatellus* (Iguanidae: Reptilia) in Puerto Rico. *Transactions of the Kansas Academy of Science* ***81***, 19 – 80 (1978)
52. Owens, A. C., & Lewis, S. M. (2018). The impact of artificial light at night on nocturnal insects: a review and synthesis. *Ecology and evolution*, *8*(22), 11337-11358.

53. Manfrin, G. Singer, S. Larsen, N. Weiß, R.H.A. Van Grunsven, N. Weiß, S. Wohlfahrt, M.T. Monaghan, F. Hölker, Artificial light at night affects organism flux across ecosystem boundaries and drives community structure in the recipient ecosystem. *Frontiers in Environmental Science* ***5***, 61 (2017)
54. A.C.S. Owens, P. Cochard, J. Durrant, B. Farnworth, E.K. Perkin, B. Seymoure, Light pollution is a driver of insect declines. *Biological Conservation* ***241***, e108259 (2020)
55. O. Levy, T. Dayan, W.P. Porter, N. Kronfeld-Schor, Time and ecological resilience: can diurnal animals compensate for climate change by shifting to nocturnal activity? *Ecological Monographs* ***89***, e01334 (2019)
56. Gao, B., Wotton, K. R., Hawkes, W. L., Menz, M. H., Reynolds, D. R., Zhai, B. P., ... & Chapman, J. W. (2020). Adaptive strategies of high-flying migratory hoverflies in response to wind currents. *Proceedings of the Royal Society B*, *287*(1928), 20200406.
57. Reynolds, D. R., Chapman, J. W., Edwards, A. S., Smith, A. D., Wood, C. R., Barlow, J. F., & Woiwod, I. P. (2005). Radar studies of the vertical distribution of insects migrating over southern Britain: the influence of temperature inversions on nocturnal layer concentrations. *Bulletin of Entomological Research*, *95*(3), 259-274.
58. Yue, M., Wang, M., Guo, J., Zhang, H., Dong, X., & Liu, Y. (2021). Long-term trend comparison of planetary boundary layer height in observations and CMIP6 models over China. *Journal of Climate*, *34*(20), 8237-8256.
59. Zhang, Y., Seidel, D. J., & Zhang, S. (2013). Trends in planetary boundary layer height over Europe. *Journal of climate*, *26*(24), 10071-10076.
60. Shahi, S., Abermann, J., Heinrich, G., Prinz, R., & Schöner, W. (2020). Regional variability and trends of temperature inversions in Greenland. *Journal of Climate*, *33*(21), 9391-9407.
61. Bell, J. R., & Shephard, G. (2024). How aphids fly: Take-off, free flight and implications for short and long-distance migration. *Agricultural and Forest Entomology*.
62. Ortega-Jiménez, V. M., & Combes, S. A. (2018). Living in a trash can: turbulent convective flows impair Drosophila flight performance. *Journal of The Royal Society Interface*, *15*(147), 20180636.

63. Reynolds, A. M., & Reynolds, D. R. (2009). Aphid aerial density profiles are consistent with turbulent advection amplifying flight behaviours: abandoning the epithet ‘passive’. *Proceedings of the Royal Society B: Biological Sciences*, *276*(1654), 137-143.
64. Wainwright, C. E., Stepanian, P. M., Reynolds, D. R., & Reynolds, A. M. (2017). The movement of small insects in the convective boundary layer: linking patterns to processes. *Scientific reports*, *7*(1), 5438.
65. Döring, T. F., & Chittka, L. (2007). Visual ecology of aphids—a critical review on the role of colours in host finding. *Arthropod-plant interactions*, *1*, 3-16.
66. Kirchner, S. M., Döring, T. F., & Saucke, H. (2005). Evidence for trichromacy in the green peach aphid, Myzus persicae (Sulz.)(Hemiptera: Aphididae). *Journal of Insect Physiology*, *51*(11), 1255-1260.
67. Lukach, M., Dally, T., Evans, W., Hassall, C., Duncan, E. J., Bennett, L., ... & Neely III, R. R. (2022). The development of an unsupervised hierarchical clustering analysis of dual-polarization weather surveillance radar observations to assess nocturnal insect abundance and diversity. *Remote Sensing in Ecology and Conservation*, *8*(5), 698-716.
68. Gauthreaux, S., & Diehl, R. (2020). Discrimination of biological scatterers in polarimetric weather radar data: Opportunities and challenges. Remote Sensing, 12(3), 545.
69. Hüppop, O., Ciach, M., Diehl, R., Reynolds, D. R., Stepanian, P. M., & Menz, M. H. (2019). Perspectives and challenges for the use of radar in biological conservation. Ecography, 42(5), 912-930.
70. Bauer, S., Tielens, E. K., & Haest, B. (2024). Monitoring aerial insect biodiversity: a radar perspective. Philosophical Transactions of the Royal Society B, 379(1904), 20230113.
71. Hu, C., Sun, Z., Cui, K., Mao, H., Wang, R., Kou, X., ... & Xia, F. (2024). Classification of biological scatters using polarimetric weather radar. IEEE Journal of Selected Topics in Applied Earth Observations and Remote Sensing.
72. D. Mirkovic, P. Stepanian, J.F. Kelly, P.B. Chilson, Electromagnetic model reliably predicts radar scattering characteristics of airborne organisms. *Scientific reports* ***6***, e35637 (2016)

73. D. Mirkovic, P. Stepanian, C.E. Wainwright, D.R. Reynolds, M.H.M. Menz, Characterizing animal anatomy and internal composition for electromagnetic modelling in radar entomology. *Remote Sensing in Ecology and Conservation* ***5***, 169 – 179 (2019)
74. F.I. Addison, T. Dally, E.J. Duncan, J.Rouse, W.L. Evans, C.Hassall, R.R. III Neely, Simulation of the radar cross section of a noctuid moth. *Remote Sensing* ***14***, e1494 (2022).

Figure 1. A) Map showing locations of 15 weather radars across the UK, and B) a 12 x 12 lattice of the different Columnar Vertical Profiles (CVPs) around the radar used for estimating aerial arthropod abundance in the present study. A) Dual polarized data from 15 UKMO-Radars (purple triangles) was processed from a fixed region around the radar (purple squares overlaid on the triangle, each corresponding to the region covered by a 12 x 12 CVP lattice as shown in B). B) Around each radar, 144 Columnar Vertical Profiles (CVPs) of 5 km diameter were generated. The spatial coordinates for each CVP were obtained by creating a regular grid with the coordinates of each radar as the centroid (golden dot in the centre). The outer black circle represents the 30 km buffer where the radar beam retains sufficient resolution for stratified height analysis. The height of the bars within each CVP corresponds to the number of voxels available across different heights (see legend for heights in meters). The number of voxels vary with the range due to the beam height and broadening, hence both the height of the bars as well as the numbers of bars is variable across CVPs. The innermost CVPs closest to the radar (within a 5 km radius; solid red circle) were removed from all downstream analysis due to highest likelihood of echoes from ground clutter. A further 12 CVPs falling within the 7.5 km radius (marked by the dashed red circle) were excluded from all radars due to insufficient vertical coverage of the radar beam. One CVP in the upper-right corner (highlighted in red) could not be processed for any radar due to technical issues.

Figure 2. Validation of radar derived estimates of arthropod abundance using a ground-based suction trap. We obtained daily total arthropod counts from a 12.2 m suction trap maintained by the Rothamsted Insect Survey, which is 17.6 km from the Chenies weather radar, and therefore within the radar's scanning range. We estimated aerial arthropod abundances for different heights in the air column, at the location of the suction trap using the methods developed in this study. We used Ordinary Least Squares (OLS) regression to assess the correlation between the observed daily arthropod abundances near the ground (from the suction trap data), and the abundance estimates obtained from the CVPs at different heights. We found strong and significant correlations between the observed arthropod abundance recorded at the suction trap, and A) abundance estimated from the Chenies weather radar, and B) ZDR or differential reflectivity. We measured the correlations at different heights within the CVP and observed that the slope of both relationships decreased with height, with the strongest relationship at lowest height. We used scaled variables for regression models since the two data are obtained at different spatial scales.

Figure 3. Temporal trends and drivers of variation for aerial diurnal and nocturnal arthropod abundances estimated over 35,000 sq. km in the UK, using UK-Met Office weather radar stations across an 8-year period. Within each plot, the values on the y-axis correspond to arthropod abundance per km^3 between 500 m and 700 m in the atmosphere (A) Cumulative abundances for diurnal (between 0800 and 1400 GMT; *shown in green*) and nocturnal (between 1800 and 2200 GMT; *shown in purple*) aerial arthropods were predicted using generalized additive models for each year between 2014 and 2021 (for raw temporal series see Fig. S3) (B-G) Each plot shows a covariate on the x-axis and aerial arthropod abundance on the y-axis. Variables shown are B) TMax: Maximum daily air temperature; C) ALAN: Artificial Light at Night measured using DN Values i.e. Digital Number which ranges from 0 to 63 where 63 represents maximum night-time illuminated sky; D-G) Percentage land cover under arable, urban, woodland and grassland. The relationships are shown for both diurnal (green) and nocturnal (purple) arthropods.

Figure 4. Spatio-temporal surfaces for diurnal (top) and nocturnal (bottom) aerial arthropod abundance estimated from UK-Met Office weather radar stations across an 8-year period in the UK. The shaded circles overlap the 15 UK weather radars for which dual polarized data was available. Aerial arthropod abundances were estimated for approximately 127 Columnar Vertical Profiles (a cylindrical volume of atmosphere, 2.5 km in radius and roughly spanning 1.8 km in height between 100-2100 m) around each radar (the shaded circles shown above are slightly enlarged for clarity). Generalized Additive Model (GAM) was used to model the spatio-temporal relationships between abundances (only between 500 and 700 m) and latitude, longitude and year. **A)** Shown here are the model outputs for only 2014 and 2021 for diurnal (top) and nocturnal (bottom) aerial arthropod abundances. **B).** Corresponds to the relative change from 2014 to 2021, with negative values indicating a decline in log(abundance/km^3) of aerial arthropods.

Figure 5. Predicted abundance densities of diurnal (shown in green; top row) and nocturnal (shown in purple; bottom row) aerial arthropods between 500 and 700 m height in the atmosphere, across the UK between 2014 and 2021. The model predictions across the entire country are derived by combining the stacked rasters of underlying covariates such as weather, land cover, elevation, and artificial light at night (ALAN), and using the modelled relationships between these covariates and arthropod abundance (as shown in Fig. 3 & 4).

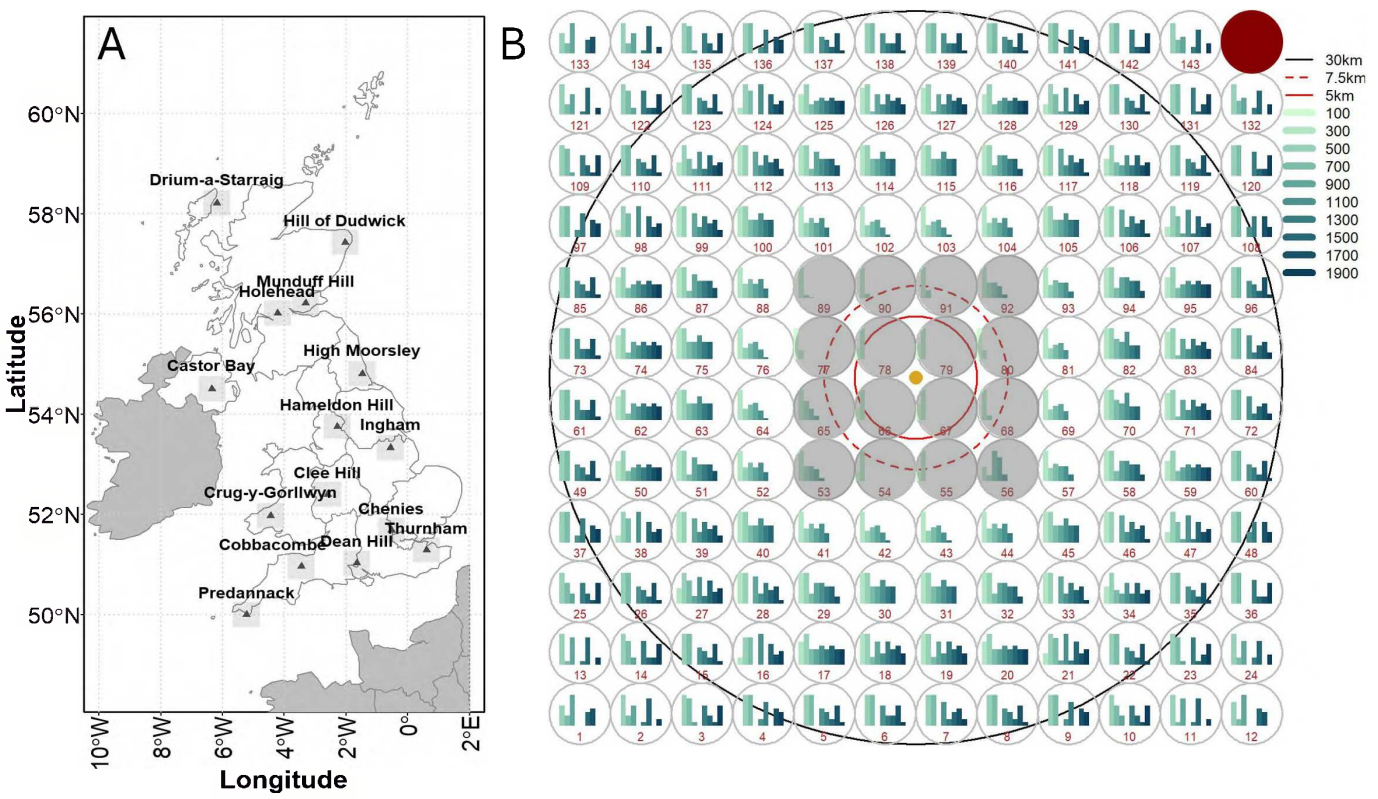
A
60°N
58°N
56°N
54°N
52°N
50°N
Latitude
10°W
8°W
6°W
4°W
2°W
0°
2°E
Longitude
Drium-a-Starraig
Hill of Dudwick
Munduff Hill
Holehead
High Moorsley
Castor Bay
Hameldon Hill
Ingham
Clee Hill
Crug-y-Gorllwyn
Chenies
Thurnham
Cobbacombe
Dean Hill
Predannack
B
30km
7.5km
5km
100
300
500
700
900
1100
1300
1500
1700
1900

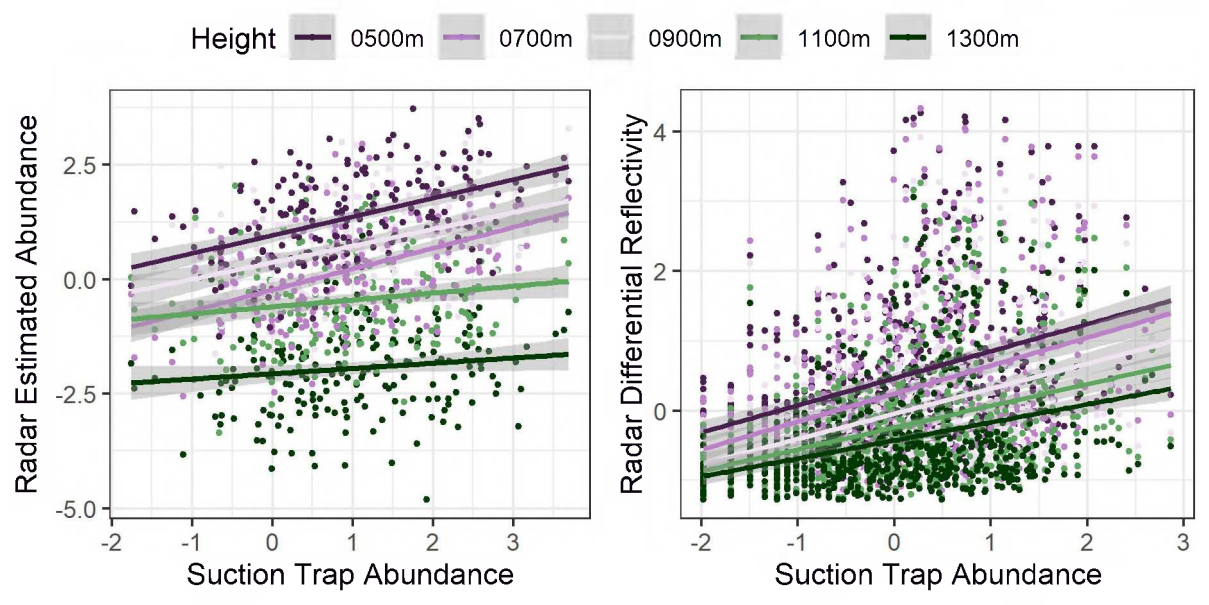
Height
0500m
0700m
0900m
1100m
1300m
Radar Estimated Abundance
2.5
0.0
-2.5
-5.0
-2
-1
0
1
2
3
Suction Trap Abundance
Radar Differential Reflectivity
4
2
0
-2
-1
0
1
2
3
Suction Trap Abundance

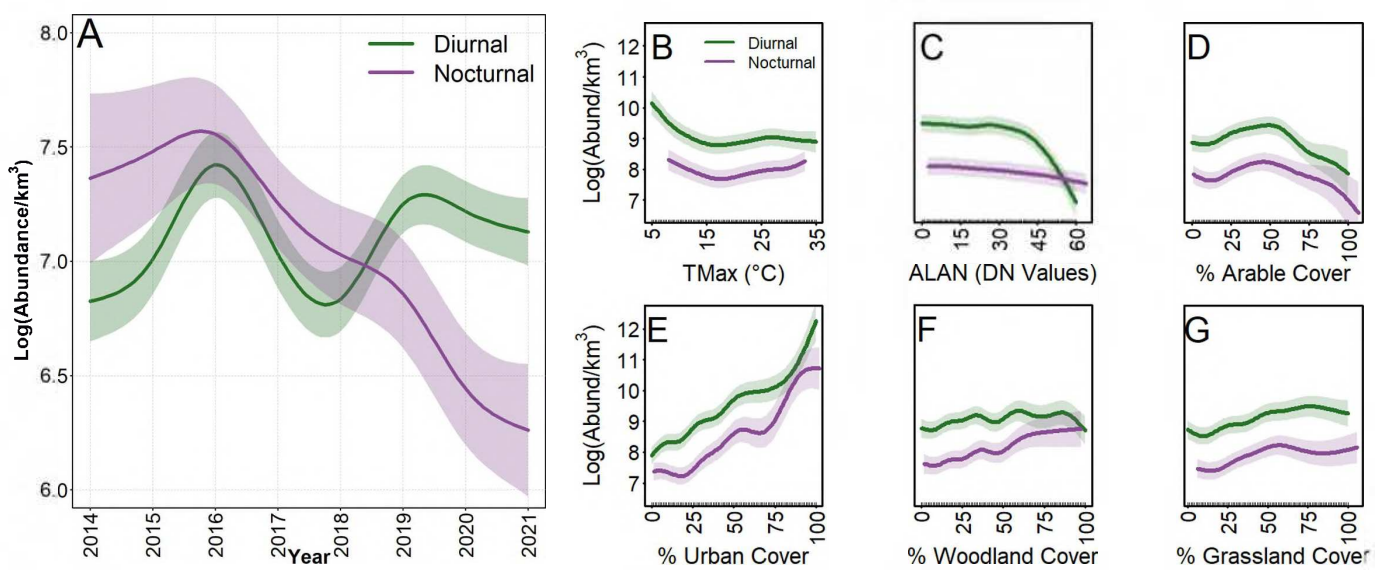
A
Diurnal
Nocturnal
Log(Abundance/km3)
8.0
7.5
7.0
6.5
6.0
2014
2015
2016
2017
2018
2019
2020
2021
Year
B
Diurnal
Nocturnal
Log(Abund/km3)
12
11
10
9
8
7
5
15
25
35
TMax (°C)
C
0
15
30
45
60
ALAN (DN Values)
D
0
25
50
75
100
% Arable Cover
E
Log(Abund/km3)
0
25
50
75
100
% Urban Cover
F
0
25
50
75
100
% Woodland Cover
G
0
25
50
75
100
% Grassland Cover

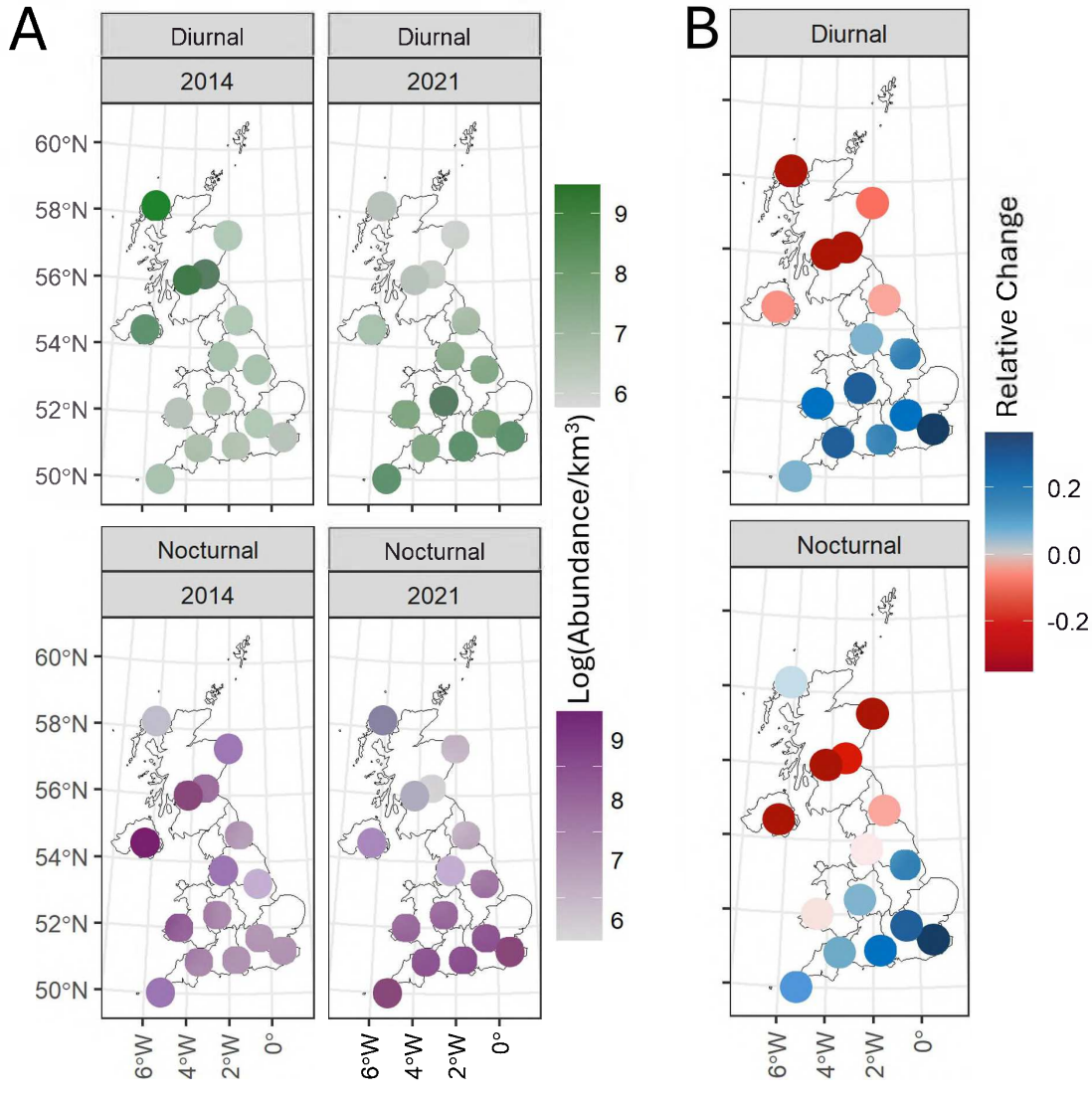
A
Diurnal
2014
Diurnal
2021
Nocturnal
2014
Nocturnal
2021
60°N
58°N
56°N
54°N
52°N
50°N
6°W
4°W
2°W
0°
Log(Abundance/km3)
9
8
7
6
B
Diurnal
Nocturnal
Relative Change
0.2
0.0
-0.2

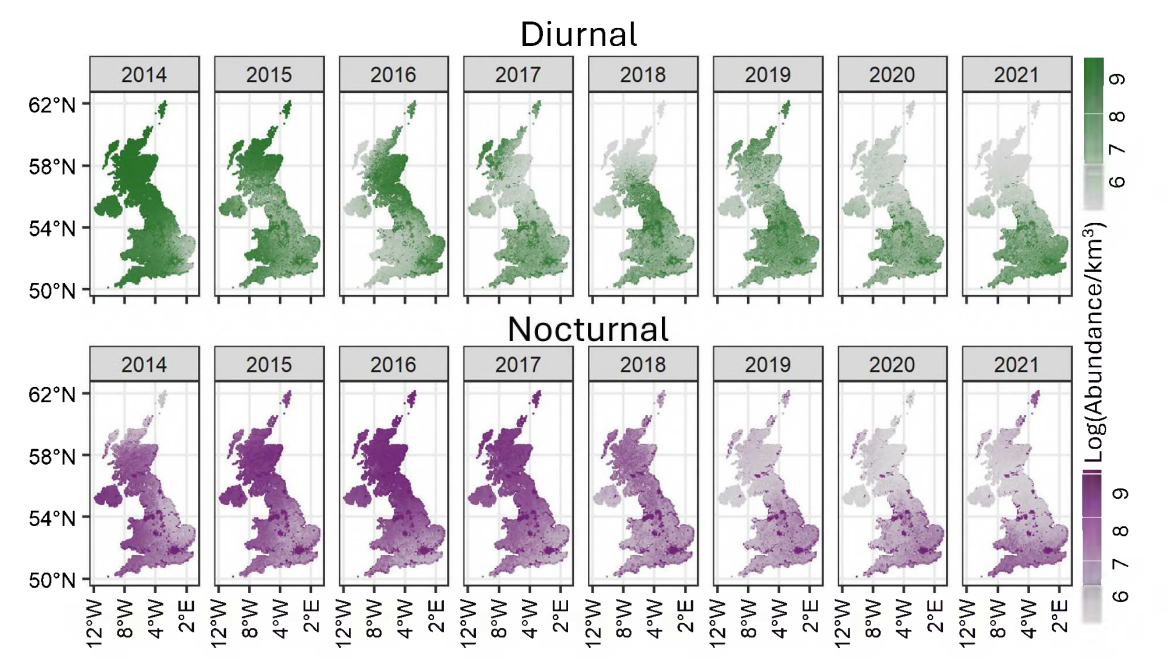
Diurnal
2014
2015
2016
2017
2018
2019
2020
2021
62°N
58°N
54°N
50°N
Nocturnal
12°W
8°W
4°W
2°E
Log(Abundance/km³)
6
7
8
9